Δελτίο της Ελληνικής Γεωλογικής Εταιρίας, 2010
Πρακτικά 12ου Διεθνούς Συνεδρίου
Πάτρα, Μάιος 2010

Bulletin of the Geological Society of Greece, 2010
Proceedings of the 12th International Congress
Patras, May, 2010

ON THE OCCURRENCE OF A VOLCANIC ASH LAYER IN THE XYLOKASTRO AREA, NORTH PELOPONNESUS, GREECE: MINERALOGY AND GEOCHEMISTRY

Vasilatos Ch.[1], Vlachou-Tsipoura M.[2], and Stamatakis M.G.[1]

[1] *National & Kapodistrian University of Athens, Faculty of Geology & Geoenvironment, Department of Economic Geology & Geochemistry, Panepistimiopolis, Ano Ilissia, 157 84 Athens, Greece, vasilatos@geol.uoa.gr, stamatakis@geol.uoa.gr*

[2] *National & Kapodistrian University of Athens, Faculty of Geology & Geoenvironment, Department of Mineralogy & Petrology, Panepistimiopolis, Ano Ilissia, 157 84 Athens, Greece, mvlachou@geol.uoa.gr*

Abstract

This paper reports, for the first time, the occurrence of an ash layer intercalated within the Plio-Pleistocene lacustrine deposits near Xylokastro area, North Peloponnesus, Greece. Petrographic and geochemical characteristics of the ash layer are the basis of this study. An attempt was made to correlate the present findings to the reported data from other ash deposits. The composition of the ash bed showed a dacitic to rhyolitic calc alkaline suit. The geochemistry of the volcanic ash indicates high crustal contamination of the lava and points to an origin from the northwest part of the Aegean volcanic arc.

Key words: *Volcanic ash, glass shards, pumice, traces element geochemistry, tephrostratgraphy, western Aegean Volcanic Arc, Greece.*

1. Introduction

Tephrochronology in its original sense is the use of tephra layers as time-stratigraphic marker beds to establish numerical or relative ages (Lowe et al., 2002). Tephra layers have been described and studied in Greece.

Because tephra beds provide essentially instantaneous chronostratigraphic marker horizons, or isochrons, that can be correlated between sites independently of radiometric dating, they provide a way of circumventing the various interpretative difficulties associated with radiocarbon dating very recent (last millennia) archaeological and paleoenvironmental (natural) sites. Because tephra deposits are found in both archaeological and natural sites, they have the capacity for linking such sites in an unambiguous manner unparalleled by other dating or correlative techniques (Lowe et al., 2000).

Identification of distinct tephra horizons in regions not traditionally associated with tephrochronological research has considerably extended the geographical distribution of some tephras, thus emphasizing the potential of using such time-parallel marker horizons for correlation of sequences on a wide scale (e.g., Turney et al., 2004).

In Northern Peloponnesus, Greece, a series of Upper Pliocene through Quaternary rocks have been deposited on a Mesozoic substrate (Koutsouveli et al., 1989). Recently, a volcanic ash layer has

been identified by the authors, hosted in clayey rocks and sandstone of Upper Pliocene to Lower Pleistocene age, located close to the eastern slopes of the Koutsa block (Place et al., 2007).

Volcanic ash beds of 4cm thick have been reported in Quaternary offshore deposits, north of the studied area (Cramp et al., 1989). Volcanic ash/tephra layers/beds have been found in sedimentary rocks of the same age in several places in eastern Mediterranean Region (Keller et al., 1978; Vinci, 1985; Stamatakis, 1995; Stamatakis et al., 2001). The majority of the Late Neogene to Recent tephra layers has their origin as either the Campanian volcanic area, or the eastern extension of the Hellenic Arc (Keller & Ninkovitch, 1972; Richardson & Ninkovitch, 1976). The aim of the present paper is to characterise the newly found volcanic ash and to consider any genetic relationship with the volcanic centers of the region.

1.1 Geological setting

The studied area is part of the Gulf of Corinth rift, which has undergone N-S extension strain, from Late Miocene through Late Quaternary (Fig. 1) (Armijo et al., 1996; Lykoussis, at al., 2007; Bell et al., 2008). Steep extensional faults (40°–50°) crop out south of the gulf, in northern Peloponnesus, mainly trending E–W, which clearly controlled the morphology of the two rift-shoulders (Sorel 2000, Place et al., 2007). The rift was created in two phases, a proto-rift stage that is well developed in the eastern part and a younger rift stage that is mostly developed in the western part (Ori, 1989).

On the Mesozoic substrate of the area which belongs to the Pindos Geotectonic Zone, clastic sediments of fluvial, lacustrine and marine origin have been deposited, having Upper Pliocene – Lower Pleistocene age (Koutsouveli et al., 1989; Doutsos and Piper, 1990). The Upper Pliocene lithostratigraphic succession is mainly composed of conglomerates, sandstones, claystones/mudstones and locally sandy marls up to 600m thick (Fig. 2). In general, the lowermost part of the deposits is more fine-grained, whereas sandstone and conglomerates predominate upwards.

The volcanic ash bed is located in the lower part of the 600m thick clastic succession, having 400m overburden sandy marls and conglomerates of the Reithio-Dendro formation (Koutsouveli et al., 1989) (Fig. 3 & 4).

2. Materials and methods

Five samples from the volcanic tephra horizon were collected from an outcrop of 15m X 50m (Fig. 2) for geochemical and mineralogical analyses. To identify the mineralogy of the host rock, five more representative samples of overlying and underlying sandstone and claystone have been collected. The sample XLK1 is the stratigraphically uppermost among the studied samples.

Grain size analyses of the bulk ash layer were performed using the sieves of 450, 320, 224, 80, 40 and 32μm. Bulk Mineralogical analysis was carried out by using an X-Ray powder Diffractometer of Siemens D-5005 type, with copper tube and graphite monochromatographer. The mineralogical phases were determined by using computer and the software of SOCABIM Company (DIFRAC PLUS 2004, EVA ver. 10) and the files of JCPDS, at the laboratories of the NKUA, Faculty of Geology and Geoenvironment.

Major and trace element chemical analysis of the bulk volcanic ash samples was implemented by ME - XRF06 (major elements) and ME - MS81 (trace and rare earth elements) methods in the laboratories of ALS Chemex Labs, Saskatchewan, Canada. Primitive mantle normalized ratios were calculated from the values of Sun & McDonough (1989).

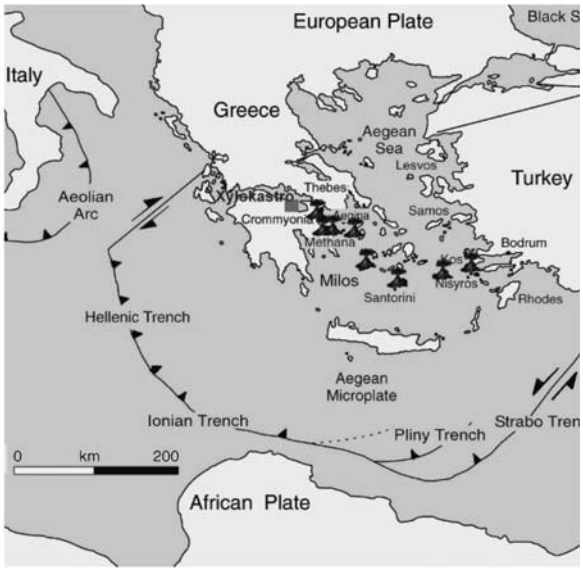

Fig. 1: Location map of the volcanic ash layer (rectangular red). Simplified regional geotectonic map of the eastern Mediterranean. The main volcanic centres of Southern Aegean Volcanic Arc [SEVA] are shown.

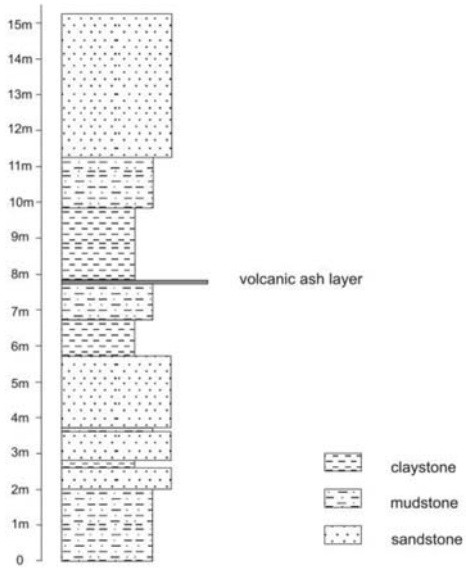

Fig. 2: Lithological column of the sedi-mentary succession that hosts the vol-canic ash-bed, Xylokastro area, Corinth.

Mineralogical, and a petrographic/scanning electron microscope survey for the volcanic ash components, i.e. glass shards, pumice particles and feldspars was performed in thin sections, using optical microscope and scanning electron microscope at the laboratories of the NKUA, Faculty of Geology and Geoenvironment. The scanning electron microscope was a JEOL JSM-5600 equipped with Oxford Link ISIS 300 Energy Dispersive microprobe analytical system. The beam current was 0.5nA and diameter 2μm. SEM and microprobe analysis were performed on slides as well as on natural samples.

Fig. 3: The ash-bed hosted in the claystone host rock. Note the tectonic deformation of the bed, due to neotectonic manifestations. Scale in inches.

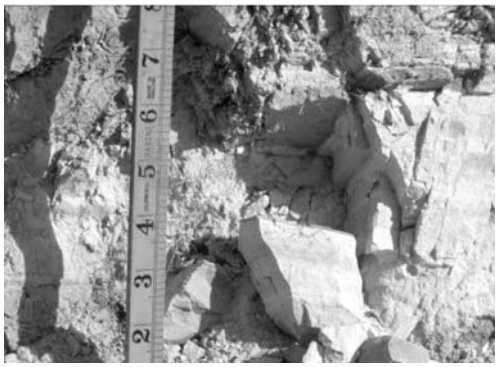

Fig. 4: A closer view of the 10cm thick ash bed showing bedding of off-white to dark grey layers.

Table 1. XRD mineralogical analysis of the volcanic ash bed and the host rock, Xylokastro area, Corinth

	Description	*VG*	*Fl*	*Qtz*	*Cc*	*Chl*	*ill-sm*
XLK-1	sandstone		MD	MJ	MD		
XLK-2	claystone		MD	MD	MD	MD	MD
XLK-3	claystone just above ash	MJ	MD	MD	TR		
XLK-4	volcanic ash	MJ	MD	TR	TR		
XLK-5 (2)	volcanic ash	MJ	MD	TR			
XLK-6 (1)	volcanic ash	MJ	MD	TR	TR		
XLK-7	volcanic ash	MJ	MD	TR			
XLK-8	volcanic ash	MJ	MD	TR			
XLK-9	claystone just below ash	MJ	MD	MD	TR		
XLK-10	mudstone		MD	MD	MD	MD	MD

Explanatory notes: VG=volcanic glass, Fl=anorthoclase and/or sanidine, Chl=chlorite, ill-sm=illite-smectite, Cc=calcite, Qtz=quartz, MJ=major constituent, MD=medium constituent, TR=minor/trace constituent

3. Results

The XRD analysis revealed that sandstone is mostly composed of quartz, feldspars and calcite, whereas mudstone and claystone contain variable amounts of calcite, quartz, feldspars, smectite, and mixed-layers. The volcanic ash bed is mostly composed of amorphous phase as it is determined by its characteristic hump at 20-26^{o} degrees. Other components that occur in minor or trace amounts are: feldspars, mostly sanidine and anorthoclase, calcite and quartz (Table 1).

The grain size distribution in the bulk ash layer is presented in Fig. 5. Chemical analyses of the volcanic ash samples revealed that they are composed primary of silica (55.80-60.74%) and alumina, (14.42-15.74%). Iron and alkalies occur in minor amounts, whereas Mg and Mn occur in trace amounts (Table 2a & b). The Harker plots (Fig. 6) shows the variation of the composition of the

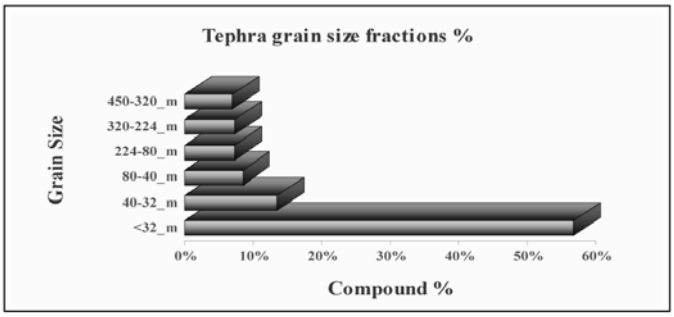

Fig. 5: Grain size distribution in the Xylokastro volcanic ash bed.

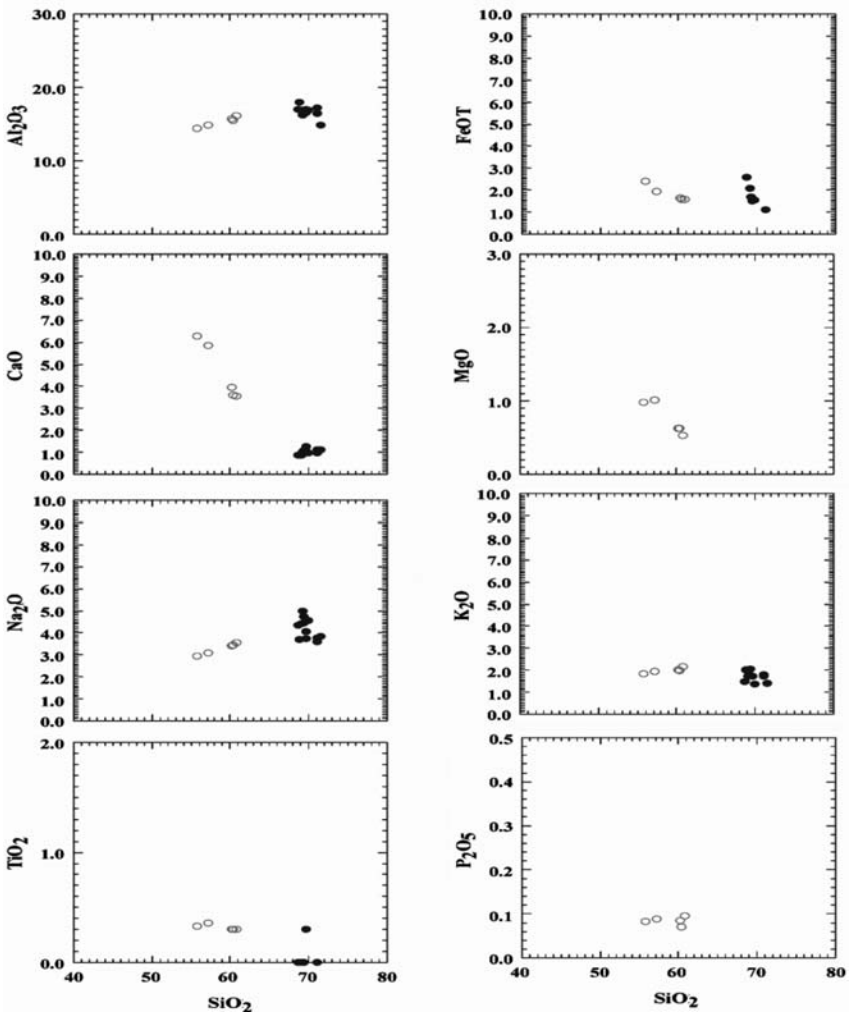

Fig. 6: Harker plots for the major elements, of the Xylokastro volcanic ash bulk samples and glass showing the variations in their composition. *(The empty cycles represent the bulk sample compositions and the full cycles the glass microprobe analyses).*

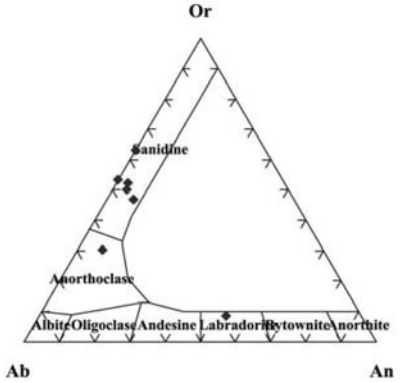

Fig. 7: Classification of the feldspars from the Xylokastro volcanic ash layer.

Table 2a. Major element analyses of bulk samples from Xylokastro tephra layer.

Sample	XLK1	XLK 1W	XLK2	XLK3	XLK4
SiO_2	57.18	60.34	55.8	60.74	60.19
TiO_2	0.36	0.3	0.33	0.3	0.3
Al_2O_3	14.84	15.5	14.42	16.11	15.74
Fe_2O_3	2.14	1.78	2.66	1.75	1.83
MnO	0.06	0.07	0.07	0.07	0.07
MgO	1.01	0.62	0.98	0.53	0.62
CaO	5.86	3.57	6.28	3.56	3.96
Na_2O	3.07	3.43	2.95	3.56	3.42
K_2O	1.94	1.96	1.83	2.14	2.03
P_2O_5	0.088	0.07	0.083	0.096	0.085
LOI	13.10	11.40	13.40	10.95	11.45
Total	99.65	99.04	98.80	99.81	99.69

Table 2b. Trace element analyses of bulk samples from Xylokastro tephra layer.

Sample	XLK1	XLK 1W	XLK2	XLK3	XLK4
Ba	650	670	560	660	680
Rb	91.7	75.4	93.7	83.3	80.6
Sr	353	324	387	390	342
Y	18.6	16.5	18.5	16.5	15.3
Zr	307	347	299	337	337
Nb	32.4	36.2	31.6	35.5	35.3
Th	88.1	87.5	89.6	86.6	79.2
Pb	125.5	136	123.5	137.5	137
Ga	21.9	23.2	20.6	21.8	22
Zn	56	49	56	46	49
Cu	21.4	11.1	23.4	9.6	11.5
Ni	56.3	28.8	59.9	19.3	28.4
V	36	29	36	26	28
Cr	39	19	33	9	17
Hf	9.6	10.9	9.4	10.6	10.6
Cs	37	40.3	35.7	39.6	39.4
Sc	3.3	2.1	3.2	1.6	1.9
Ta	1.56	1.72	1.54	1.73	1.73
Co	7.2	4.5	7.5	3.5	4.4
Li	22.6	12.8	21.8	11.5	12.2
Be	11.95	13.55	11.5	13.2	13.1
U	21.3	22.3	20.6	21.7	21
W	11	12.7	10.5	12.3	12.2
Sn	3.4	3.9	3.4	3.7	3.6
Mo	7.87	8.32	7.3	7.36	7.39
La	86.1	71.3	91	70.3	63.6
Ce	145.5	127	150	125.5	113.5
Th/U	4.14	3.92	4.35	3.99	3.77

Table 3. Representative microprobe analyses of volcanic glass particles.

Analysis	S4	S7	X10	X11	X6	X7	X8	X9
SiO_2	68.77	71.59	69.26	69.04	68.68	69.43	71.07	69.65
TiO_2	0.00	0.00	0.00	0.00	0.00	0.00	0.00	0.30
Al_2O_3	17.95	14.89	16.25	16.85	17.00	16.48	16.46	17.00
FeO	1.75	1.98	1.69	2.08	2.60	1.51	1.12	1.55
CaO	0.85	1.10	1.02	0.88	0.88	1.08	0.99	1.04
Na_2O	3.69	3.83	5.00	4.40	4.35	4.44	3.57	3.73
K_2O	2.00	1.42	1.78	1.74	1.49	2.06	1.80	1.73
Total	95.01	94.81	95.00	94.99	95.00	95.00	95.01	95.00

Table 4. Representative microprobe analyses of feldspars from the ash layer.

Analysis	S10	S12	S13	S5	S6	S9	X5	X5A
SiO_2	69.04	66.45	62.89	67.55	69.06	68.73	68.73	69.87
Al_2O_3	17.64	19.63	17.99	17.98	17.62	17.12	17.98	17.1
FeO	0.00	0.00	4.11	0.00	0.00	0.87	0.00	1.88
CaO	0.00	1.45	8.46	0.86	0.00	0.00	0.61	1.15
Na_2O	4.86	4.87	3.38	5.11	4.86	3.67	4.56	5.56
K_2O	8.46	7.60	1.17	8.49	8.46	9.56	8.12	4.08
Total	100.00	100.00	98.00	99.99	100.00	99.95	100.00	99.64

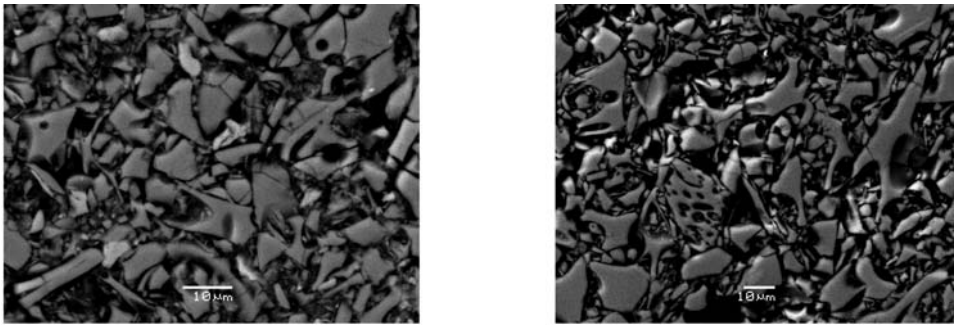

Fig 8a: SEM images of the Xylokastro ash bed: Glass shards. Note the fineness of the particles [size <20μm].

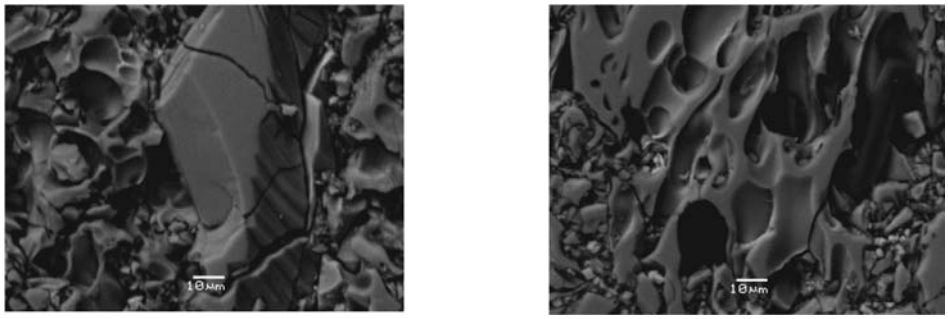

Fig. 8b: SEM images of the Xylokastro ash bed: Pumice and feldspar fragments [left image]. The particle size of both components is higher than that of the glass shards.

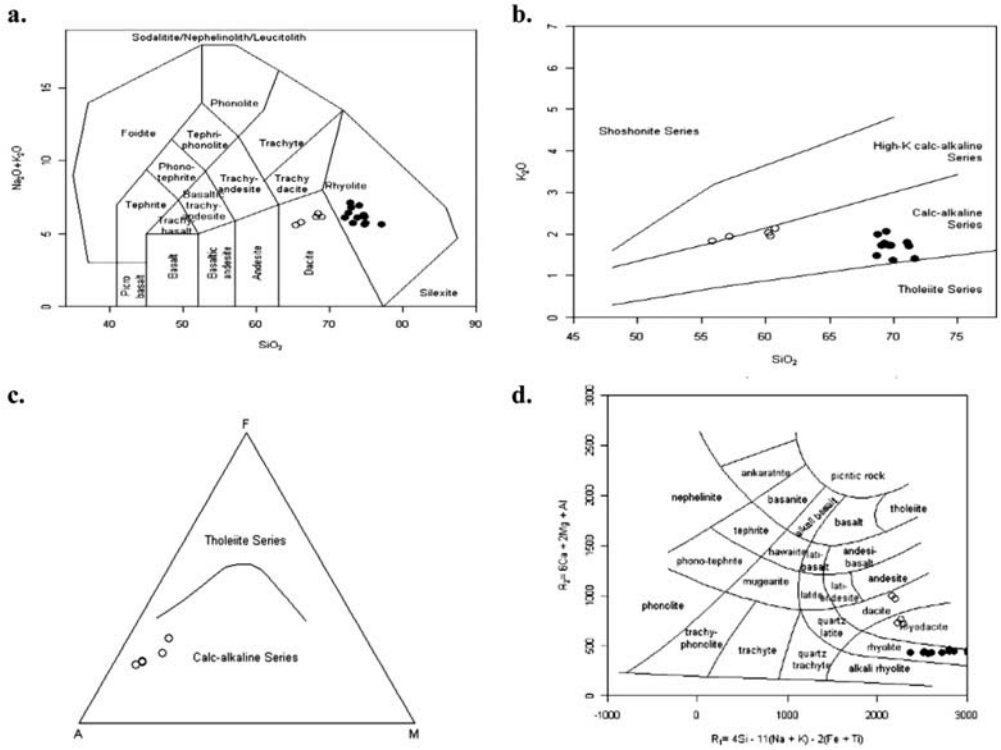

Fig. 9: Geochemical discrimination dia-grams for the Xylokastro volcanic ash bulk samples and glass: a. TAS classification diagram (Middlemost, 1994), b. SiO_2 - K_2O binary classification diagram of Pecerillo & Taylor, (1976), c. AFM ternary classification diagram of Irvine & Baragar, (1971). A.: Na_2O+K_2O, F: FeOt, M: MgO, d. R1-R2 binary classification plot (De la Roche et al, 1980). The empty cycles represent the bulk sample compositions and the full cycles the glass microprobe analyses.

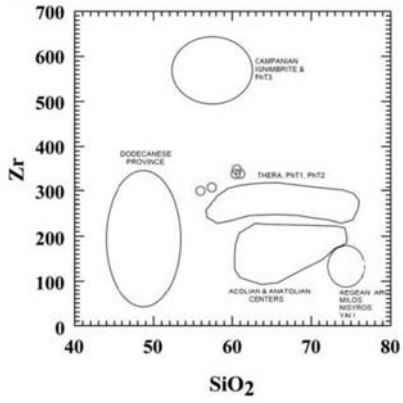

Fig. 10: The Xylokastro ash-bed [red circles] in the Zr vs. SiO_2 systematics (after Seymour et al., 2004).

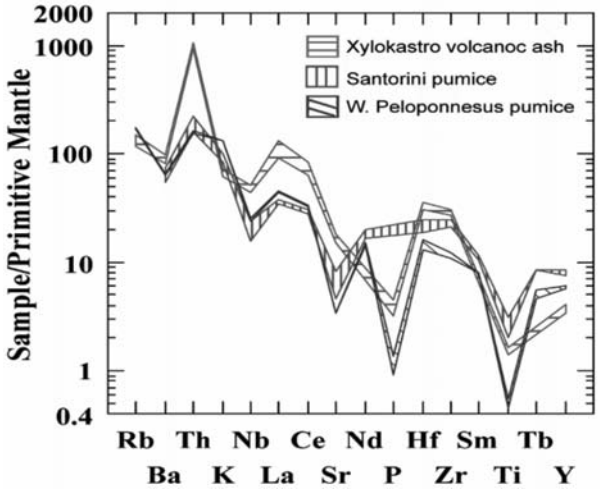

Fig. 11: Trace element spider plots of the Xylokastro volcanic ash bulk samples, Thera [Santorini] pumices (data from Vitaliano et al., 1989), and. pumices from western Peloponnesus (data from Bathrellos et al., 2009).

Xylokastro volcanic ash bulk samples and glass for the major elements. The higher CaO values in the bulk samples is most likely due to trace amounts of calcite (Table 1), but mainly to an early crystallization of Ca- and Mg-rich mafic minerals in the melting lava. This suggestion is supported by the simultaneous negative trend of MgO versus SiO_2 (Fig. 6).

The study of the samples by SEM presented good sorting, without any evidence of compaction and restricted transportation, as there is no abrasion evidence on grains, fragmentation of glass shards. The diatom frustules that rarely occur in the ash bed retain their minute structure, being preserved unbroken. Microprobe analyses of volcanic glass particles and feldspar crystals are shown in Tables 3 & 4 respectively. The classification of the feldspars of the samples is presented in Fig. 7. showing that the dominant feldspar is sanidine and also the presence of anorthoclase and plagioclase. The SEM-EDS observations suggested slight alteration of both the glass shards and the pumice particles (Fig. 8a & b). The common alteration sequence detected, is the following: 1) etching on glass-grain surfaces 2) formation of silica spheres and quartz overgrowths 3) precipitation of very thin, individual flakes of illite-smectite on glass shards or development of illite-smectite aggregates filling pores 4) formation of Fe-oxides rim along cracks and in voids 5) alteration on plagioclase crystals. The glass fractions consist of shards, bubble wall fragments and micro-particles of pumices. Glass shards show typical conhoidal fracture and different particle shape. Many shards exhibit characteristic U- and Y-shapes (tri-cuspate) that have resulted from disruption of highly vesicular pumices that were formed where three bubbles were in close proximity. Other shard derived of double –concave plates that formed the wall between two adjoining bubbles, whereas some particles are angular and lenticular, or highly vesicular. The vesicles, spherical or elongated, have been arranged in groups and in some cases they are curved.

4. Discussion and Conclusions

Mineral and chemical composition is used in the description of volcanic ash deposits. Description of particle size and shape as well as the types of vesicles are also used in ash petrography. The type of material present in volcanic ash is a function of a) the kind of source rock emitted, b) the modification by transport and contamination during transport or deposition c) the alteration processes (devitrification and/or weathering).

The studied samples of the distinct volcanic ash layer, reported for the first time in the studied area, seem to have been deposited in a lacustrine environment displaying parallel-laminated fine tuff layers, possibly formed by subaqueous pyroclastic flows that are generated by eruptions in shallow water or close to a shore. The lacustrine nature of the deposit is determined by the examination of the diatom species found in the volcanic ash and the host rock (*Cyclotella Sp*., Prof. B. Owen). Its main components are glass shards and pumice particles. According to Izett et al (1981), pumice shard develop from relatively high viscous rhyolitic magmas with temperature <850° C, whereas the bubble wall and bubble junction shards develop from low viscosity rhyolitic magmas at temperature >850° C. Their coexisting in the ash layer could be attributed to successive eruptions, or settling velocity or/and disturbance. The cooling-contraction fragmentation of shard glass points out to ash/water interaction Kokelar (1986). The homogeneous fine-grained, well-sorted and parallel laminated ash layers are products of either a single volcanic event from a subaqueous flow that dispersed in the water column, or distant eruption. In the latter case, the homogeneity is produced by winnowing during aerial transport. The Xylokastro ash has shown a greater percentage of bubble wall shards with the co-occurrence of blocky types as compared to pumice shard. Rose and Chesner (1987) have pointed to the high drag coefficient of the bubble wall shard which resulted in its preferential dispersal over great distances.

The XRD analysis of the finest [<32μm, off-white] and the coarser fraction [450-320μm dark grey] of the volcanic ash particles showed that there does no any difference in their mineralogy, hence the difference in the color is attributed to differential grain size. The lamination observed in the field is due to the alternation of coarse-rich and fine-rich intercalations in the ash. The thickness of each micro-layer is variable but always <2cm, comparing the dark and bright intervals. Moreover, the bright and dark layers themselves most likely propose repetitive volcanic manifestations in a certain/short period of time, or almost simultaneous manifestations of neighbouring volcanoes that fed the area with successively deposited sheets of ash.

The ash layers have undergone and early alteration processes that refer to the effects of devitrification and/or weathering. Altered glass shards are characterized by silica remobilization and development of sorptive phases as clay minerals. The devitrification process is not intense, as the surfaces of glass shards remain relatively fresh, and the alteration products are rare. It is also confirmed by the Th/U ratio [~4] which displays no uranium-loss attributed to devitrification (Table 2).

The composition of the bulk samples showed a dacitic to rhyodacitic calc alkaline suit with relative high potassium (fig. 9). The glass itself has more silicic composition than the bulk sample (fig. 6) indicating a rhyolitic, calk alkaline suit as well (fig. 9). This difference is probably due to the mineralogy of the bulk samples, which contain minerals with variable SiO_2 content (Table 1).

In the binary diagram Zr versus SiO_2 - systematics proposed by Seymour et al. (2004), the bulk sample composition is plotted a little above the field of Santorini pyroclastics (fig. 11). The fineness of the glass and pumice particles (fig. 5), judges for a rather long distance source of the volcanic material.

As it was pointed out by Fischer (1965), in areas of successive eruptions and water sedimentation feldspar or quartz may reach the water bottom at the same time as glass shards from a previous eruption, due to differential settling velocity. The spider area plots for the trace element composition (Fig. 11) shows similarity with the trace element area plots of Santorini pumices and the newly found western Peloponnesus pumices which are assumed to originate from the Aegean volcanic arc (Bathrellos et al., 2008). The differences between those plots are due to a) the lack of analytical date for some elements in each group, b) the higher thorium content of the Xylokastro tephra, which is

accompanied by high uranium value (Table 2) and c) Xylokastro tephra shows higher enrichment in LIL elements than the others. Magma-crust interaction is an explanation for the high LIL/HFS element in calc-alkaline magmas (Mitropoulos et al., 1987). Differential crustal assimilation could account for the geochemical differences between the Aegean volcanic centers and may be interpreted as evidence for slightly higher sediment input in the western parts of the arc. Among the volcanic centers of the SEVA, Santorini is situated in the region which has suffered maximum crustal thinning and lithosphere extension, and where asthenospheric mantle may be uprising to replace existing sub-continental mantle. The crust and lithosphere thickness is higher in the margins of SAVA. Xylokastro volcanic ash having enrichment in LIL elements indicates high crustal contamination of the lava and points to an origin from the northwest part of the Aegean volcanic arc (Methana, Aegina, Poros, Sousaki (Cromyonia) or neighbouring volcanic centers, not exposed today). However, among the possible feeding centers is the Soussaki volcanic terrain is the closest, lying 50 Km eastwards.

5. Acknowledgments

The authors would like to thank Prof. P. Mitropoulos of the University of Athens and Assoc. Prof. K. Seymour of the University of Patras, Geochemists, for their useful remarks for the interpretation of the geochemical data. Also thanks, to Dr K. Kouli for her help in electronic drawing the lithostratigraphic column of the study area.

6. References

Armijo, R., Meyer, B., King, G.C.P., Rigo, A., Papanastasiou, D., 1996. Quaternary evolution of the Corinth rift and its implications for Late Cenozoic evolution of the Aegean. *Geophys. J. Int.* 126, 11–53.

Bathrellos D.G.,, Vasilatos Ch., Skilodimou D.H., Stamatakis G.M., 2009. On the occurrence of a pumice-rich layer in Holocene deposits of western Peloponnesus, Ionian Sea, Greece. A geomorphological and geochemical approach. *Cent. Eur. J. Geosci.*, 1(1) , 19-32.

Bell R. E., McNeill L.C., Bull M.G. and Henstock J.T. 2008. Evolution of the offshore western Gulf of Corinth. *Geological Society of America Bulletin*, V. 120, p. 156-178.

Cox, K.G, Bell, J.D, Pankhurst, R.J., The interpretation of igneous rocks. Allen and Unwin, London, UK, 1979.

Cramp A., Vitaliano J. C. Collins B. M. 1989. Identification and Dispersion of the Campanian Ash Layer (Y-5) in the Sediments of the Eastern Mediterranean. *Geo-Marine Letters* V. 9, p. 19-25

De La Roche, H., 1980. A classification of volcanic and plutonic rocks using R1–R2 diagrams and major element analyses—its relationships and current nomenclature, *Chem. Geol.* 29, pp. 183–210.

Doutsos, T., Piper, D.J.W., 1990. Listric faulting, sedimentation and morphological evolution of the Quaternary eastern Korinth rift, Greece; first stages of continental rifting. *GSA Bull.* 102, 819–879.

Irvine, T.N., Baragar, W.R.A., 1971. A guide to the chemical classification of the common volcanic rocks, *Canadian Journal of Earth Science*, 8, 523 – 548.

Izett, G.A., 1981. Volcanic ash beds: recorders of upper Cenozoic silicic pyroclastic volcanism in the western U.S. *Journal of Geophysical Research* 86, pp. 10,200–10,222.

Fischer R.V. 1965. Settling velocity of shard glass. Deep Sea Research and Oceanographic Abstracts. 12,3, 345-346.

Ori, G.G., 1989. Geological history of the extensional basin of the gulf of Corinth (?Miocène–Pleistocène), Greece. *Geology* V. 17, p. 918–921.

Pecerillo, A. and Taylor, S.R., 1976. Geochemistry of Eocene calc-alkaline volcanic rocks from the Kas-

tamonu area, northern Turkey. *Contrib. Mineral. Petrol.* 58, pp. 63–81.

Place J., Géraud Y., Diraison M., Warr L. 2007. North-south transfer zones and paleo-morphological reconstruction of the Xylokastro area (Corinth Gulf, Greece). *Tectonophysics* V. 440, p. 121–139

Richardson and D. Ninkovich, 1976. Use of K_2O, Rb, Zr and Y versus SiO_2 in volcanic ash layers of the Eastern Mediterranean to trace their source, *Geol. Soc. Am. Bull.* 87, pp. 110–116.

Sorel D. 2000. A Pleistocene and still-active detachment fault and the origin of the Corinth-Patras rift, Greece. *Geology*, V. 28; no. 1; p. 83-86.

Keller and D. Ninkovich, 1972. Tephra-Lagen in der Agäis. *Z. Dtsch. Geol. Ges.* 123, pp. 579–587.

Keller, W.B.F. Ryan, D. Ninkovich and R. Altherr, 1978, Explosive volcanic activity in the Mediterranean over the past 200,000 yr as recorded in deep-sea sediments, *Geol. Soc. Am. Bull.*, 89 pp. 591–604.

Kokelar P. 1986, Magma-water interactions in subaqueous and emergent basaltic volcanism. *Bull. of Volcanology* 48, 275-289.

Koutsouveli, A., Mettos, A., Tsapralis, V., Tsaila-Monopoli S., Ioakim, C., 1989. Geological Map of Greece, scale 1:50000, Xylokastro sheet, IGME publications, Greece.

Lowe, D.J., Newnham, R.M., McFadgen, B.G. and Higham, T.F.G., 2000: Tephras and New Zealand archaeology. *Journal of Archaeological Science*, 27, 859-870.

Lowe, D.J., Newnham, R.M. and McCraw, J.D., 2002: Volcanism and early Maori society in New Zealand. In: Natural Disasters and Cultural Change; Torrence, R. and Grattan, J. (eds), Routledge, 126-161

Lykousis V. Sakellariou D., Moretti I, and Kaberi H., 2007. Late Quaternary basin evolution of the Gulf of Corinth: Sequence stratigraphy, sedimentation, fault–slip and subsidence rates. *Tectonophysics*, V, 440, issues 1-4, p. 29-51.

Middlemost, K.A.E,. 1994. Naming materials in the magma/igneous rock system, *Earth-Science Reviews* 37, pp. 215–224.

Mitropoulos P., Tarney J., Saunders A. D., and Marsh N. G., 1987. Petrogenesis of Cenozoic volcanic rocks from the Aegean island arc. *Journal of Volcanology and Geothermal Research* 32, p. 177-193.

Ori, G.G., 1989. Geological history of the extensional basin of the gulf of Corinth (?Miocène–Pleistocène), Greece. *Geology* V. 17, p. 918–921.

Rose W.I. and Chesner C.A. 1987: Dispersal of ash in the great Toba eruption. *Geology* 15, 913-917.

Sun S.S., McDonough W.F., 1989. Chemical and isotopic systematics of oceanic basalts: implications for mantle composition and processes. In: Saunders, A.D., Norry, M.J. (Eds.), Magmatism in the Ocean Basins. *Geological Society Special Publications*, pp. 313–345.

Seymour, K., Christanis, K., Bouzinos, A., Papazisimou, St., Papatheodorou, G., Moran, E. & Denes, G., 2004. Tephrostratigraphy and tephrochronology in the Philippi peat basin, Macedonia, Northern Hellas (Greece), *Quatern. Internat.*, 121, 53 – 65.

Stamatakis M.G. 1995. Occurrence and genesis of huntite-hydromagnesite assemblages, Kozani basin, Greece - important new white fillers and extenders. 1995. IMM, *Transactions B*, V 104, p. 179-186.

Stamatakis M.G., Papageorgiou A., Fragoulis D. & Chaniotakis E. 2001. The nature of volcanic glass and its effect in the pozzolanic activity of tuffaceous rocks originated from Macedonia, Northern Greece. Proceedings of the 8th Euroseminar on Microscopy Applied to Building Materials. V. 1, p. 271-280.

Turney, C.S.M., Lowe, J.J., Davies, S.M., Hall, V.A., Lowe, D.J., Wastegård, S., Hoek, W.Z., Alloway, B., SCOTAV and INTIMATE members, 2004: Tephrochronology of Last Termination sequences in Europe: a protocol for improved analytical precision and robust correlation procedures (a joint SCOTAV-INTIMATE proposal). *Journal of Quaternary Science* 19, 111-120.

Vinci, A., 1985. Distribution and chemical composition of tephra layers from Eastern Mediterranean abyssal sediments. *Marine Geology*, Volume 64, Issues 1-2, pp 143-155

Vitaliano, C.J., Taylor, S.R., Norman, M.D., McCulloch, M.T., Nicholls, I.A., 1989 Ash layers of the Thera volcanic series: stratigraphy, petrology, and geochemistry. Thera and the Aegean World III. Papers to be presented at the 3nd International Congress, Santorini, Greece 3–9 September 1989. Volume I sessions 1–3, pp. 115–150.